TU Clausthal
Clausthal University of Technology

The Class of Simo & Pister-type Hyperelasticity Relations

Stefan Hartmann

Technical Report Series Fac3-10-02

Faculty of
Mathematics/Computer Science
and Mechanical Engineering
Clausthal University of Technology

Impressum

Publisher: Fakultät für Mathematik/Informatik und Maschinenbau,
Technische Universität Clausthal
Am Regenbogen 15, 38678 Clausthal-Zellerfeld, Germany
Editor-in-chief: Alfons Esderts
Technical editor: Martina Wächter
Contact: martina.waechter@tu-clausthal.de
URL: http://www.fakultaet3.tu-clausthal.de/forschung/technical-reports/
ISSN: 1869-8018

The Class of Simo & Pister-type Hyperelasticity Relations

Stefan Hartmann

Institute of Applied Mechanics, Clausthal University of Technology, Adolph-Roemer-Str. 2a, 38678 Clausthal-Zellerfeld, Germany, stefan.hartmann@tu-clausthal.de

Abstract

A finite strain hyperelasticity relation, which is frequently utilized in the field of Computational Mechanics, has been proposed by [Simo and Pister, 1984]. The original strain-energy function of this elasticity relation can be modified so that a general representation is obtained. Accordingly, particular studies of the properties of the original and further strain-energy functions are necessary. This includes both the derivation of the stress computation and the consistent tangent operator within non-linear finite element analysis and simple homogeneous deformations such as simple tension/compression and simple shear. The latter case of simple homogeneous deformations are required as testing examples in the verification step of the more general verification and validation process.

1 Introduction

Although a huge number of constitutive models in finite strain elasticity have been published so far, even the most famous are not investigated in detail. Hyperelasticity relations in the finite strain regime are used for modeling the pure elastic response or they are embedded in models developed in finite strain viscoelasticity, plasticity or viscoplasticity (see [Lion, 1996, Reese and Govindjee, 1998, Hartmann, 2002, Lührs et al., 1997] and the literature cited therein). The necessity of detailed investigations on the analytical level was shown by [Ehlers and Eipper, 1998], since there exist models showing that even in simple tension a specimen becomes thicker after a certain amount of axial stretching (or it gets thinner in compression), [Hartmann and Neff, 2003]. This, however, contradicts our daily experience. Furthermore, simple analytical and half-analytical examples are necessary for code verification purposes representing one of the verification steps in the verification and validation concepts (see [Roache, 1998, Schwer, 2001]). Here, it is thought of verifying finite element implementations, which is one of the most often applied numerical method in engineering applications.

In view of the verification and validation step the stress computation is treated and the consistent linearization, which is necessary in a Newton-like iteration scheme in finite elements, is appended. For code verification two simple deformations, namely simple tension and simple shear, are proposed. Particularly, simple shear turns out to be investigated in more detail for both the finite element discretization and for the constitutive model applied here.

The investigations are carried out at a frequently applied material model proposed by [Simo and Pister, 1984]. It will turn out that this model shows some physical drawbacks.

2 Model description

In the following, the basic ideas and properties of the Simo & Pister-type hyperelasticity models are summarized, where further topics are discussed. In this respect, we refer to the original literature, [Simo and Pister, 1984]. This class of hyperelasticity relations are based on a strain-energy function of the type

$$\psi(J, \mathrm{I_C}) = \overline{U}(J) + w(\mathrm{I_C}) = U(J) - \mu \ln J + \frac{\mu}{2}(\mathrm{I_C} - 3), \tag{1}$$

where $J = \det \mathbf{F}$ defines the determinant of the deformation gradient $\mathbf{F} = \operatorname{Grad} \vec{\chi}_{\mathrm{R}}(\vec{X}, t)$, $\vec{x} = \vec{\chi}_{\mathrm{R}}(\vec{X}, t)$ symbolizes the motion of a material point $\vec{X}$, and $\mathrm{I_C} = \operatorname{tr} \mathbf{C}$ is the first invariant of the right Cauchy-Green tensor $\mathbf{C} = \mathbf{F}^T\mathbf{F}$. $\operatorname{tr} \mathbf{A} = a_k^k$ denotes the trace operator. In other words,

$$\overline{U}(J) = U(J) - \mu \ln J, \qquad w(\mathrm{I_C}) = \frac{\mu}{2}(\mathrm{I_C} - 3) \tag{2}$$

$$\overline{U}'(J) = U'(J) - \frac{\mu}{J}, \qquad w'(\mathrm{I_C}) = \frac{\mu}{2} \tag{3}$$

$$\overline{U}''(J) = U''(J) + \frac{\mu}{J^2}, \qquad w''(\mathrm{I_C}) = 0 \tag{4}$$

hold, with the property $\overline{U}(1) = 0$ and $w(3) = 0$ (strain-energy free undeformed configuration). In the original paper the strain-energy

$$U(J) = \frac{\Lambda}{2}(\ln J)^2, \quad U'(J) = \Lambda\frac{\ln J}{J}, \quad U''(J) = \Lambda\frac{1 - \ln J}{J^2}. \tag{5}$$

is defined. In the investigations carried out here, we do not specify the strain-energy part $U(J)$ at the moment and look for those described in the literature. A number of functions $U(J)$, which have been proposed in connection with strain-energy functions decomposed into volume-preserving and volume-changing parts, are summarized, see Tab. 1, see [Hartmann and Neff, 2003]. Usually, these parts of the strain-energy function are applied in the context of models based on the multiplicative decomposition of the deformation gradient into an isochoric and a volumetric part. In this respect, the original Simo & Pister model can be modified by changing the strain-energy part $U(J)$, even though it fits not into this class of models.

First, the three-dimensional stress calculation and the related consistent linearization are summarized. The second Piola-Kirchhoff tensor $\mathbf{S} = J\mathbf{F}^{-1}\boldsymbol{\sigma}\mathbf{F}^{-T}$ reads in the case of hyperelasticity, see [Truesdell and Noll, 1965, Ogden, 1984, Haupt, 2002],

$$\mathbf{S} = 2\frac{\mathrm{d}\psi}{\mathrm{d}\mathbf{C}} = 2\overline{U}'(J)\frac{\mathrm{d}J}{\mathrm{d}\mathbf{C}} + 2w'(\mathrm{I_C})\frac{\mathrm{d}\mathrm{I_C}}{\mathrm{d}\mathbf{C}} = \tag{6}$$

$$= \overline{U}'(J)J\mathbf{C}^{-1} + \mu\mathbf{I}, \tag{7}$$

Table 1: Various strain-energy functions $U(J)$ (see [Hartmann and Neff, 2003])

$U(J)/\Lambda$	$U'(J)/\Lambda$	$U''(J)/\Lambda$	Reference
$\frac{1}{2}(J-1)^2$	$J-1$	1	
$\frac{1}{4}\left((J-1)^2+(\ln J)^2\right)$	$\frac{1}{2}\left(J-1+\frac{1}{J}\ln J\right)$	$\frac{1}{2J^2}(1+J^2-\ln J)$	[Simo and Taylor, 1982]
$\frac{1}{2}(\ln J)^2$	$\frac{1}{J}\ln J$	$\frac{1}{J^2}(1-\ln J)$	[Simo et al., 1985]
$\frac{1}{\beta^2}\left(\frac{1}{J^\beta}-1+\beta\ln J\right)$	$\frac{1}{\beta}\left(\frac{1}{J}-\frac{1}{J^{1+\beta}}\right)$	$\frac{1}{\beta}\left(\frac{1}{J^{2+\beta}}(1+\beta-J^\beta)\right)$	[Ogden, 1972]
$\frac{1}{4}\left(J^2-1-2\ln J\right)$	$\frac{1}{2}\left(J-\frac{1}{J}\right)$	$\frac{1}{2}\left(1+\frac{1}{J^2}\right)$	[Simo and Taylor, 1991]
$J-\ln J-1$	$1-\frac{1}{J}$	$\frac{1}{J^2}$	[Miehe, 1994]
$J^\beta(\beta\ln J-1)+1$	$\beta^2\frac{1}{J^{1-\beta}}\ln J$	$\beta^2 J^{\beta-2}(1+(\beta-1)\ln J)$	[Hartmann, 2002]
$J\ln J-J+1$	$\ln J$	$\frac{1}{J}$	[Liu et al., 1994]
$\frac{1}{32}(J^2-J^{-2})^2$	$\frac{1}{8}\left(J^3-\frac{1}{J^5}\right)$	$\frac{1}{8}\left(5\frac{1}{J^6}+3J^2\right)$	[ANSYS, 2000]
$\frac{J}{\beta}\left(1-\frac{J^{-\beta}}{1-\beta}\right)+\frac{1}{\beta-1}$	$\frac{1}{\beta}\left(1-J^{-\beta}\right)$	$J^{-(1+\beta)}$	[Murnaghan, 1951, S.68]
$\frac{1}{50}\left(J^5+J^{-5}-2\right)$	$\frac{1}{10}\left(J^4-J^{-6}\right)$	$\frac{1}{10}\left(4J^3+6J^{-7}\right)$	[Hartmann and Neff, 2003]

where $\boldsymbol{\sigma}$ is the Cauchy stress tensor and $\mathbf{I}$ defines the identity tensor of second order. Here, the relations

$$\frac{\mathrm{d}J}{\mathrm{d}\mathbf{C}}=\frac{1}{2}J\mathbf{C}^{-1} \qquad \text{and} \qquad \frac{\mathrm{d}\mathrm{I}_\mathbf{C}}{\mathrm{d}\mathbf{C}}=\mathbf{I} \tag{8}$$

have been exploited. In order to obtain quantities operating on the current configuration, the push-forward operator $\mathcal{F}=[\mathbf{F}\otimes\mathbf{F}]^{T_{23}}$ is applied, which leads to the Cauchy stress tensor

$$\boldsymbol{\sigma}=\frac{1}{J}\mathcal{F}\mathbf{S}=\frac{1}{J}\mathbf{F}\mathbf{S}\mathbf{F}^T=\overline{U}'(J)\mathbf{I}+\frac{\mu}{J}\mathbf{B} \tag{9}$$

with the left Cauchy-Green tensor $\mathbf{B}=\mathbf{F}\mathbf{F}^T$.

Second, the consistent tangent operator concerned has to be investigated. The consistent linearization step is reckoned by applying the Gateaux-derivative ($\mathsf{D}_\mathbf{A}\,\mathbf{h}(\mathbf{A})[\mathbf{H}]=\frac{\mathrm{d}}{\mathrm{d}\lambda}\mathbf{h}(\mathbf{A}+\lambda\mathbf{H})|_{\lambda=0}$) of the elasticity relation (7)

$$\tilde{\mathcal{C}}\mathbf{H}=2\mathsf{D}_\mathbf{C}\,\mathbf{S}(\mathbf{C})[\mathbf{H}]=2\frac{\mathrm{d}\mathbf{S}}{\mathrm{d}\mathbf{C}}\mathbf{H}, \tag{10}$$

leading to

$$\tilde{\mathcal{C}}=\left(\overline{U}''(J)J^2+\overline{U}'(J)J\right)\mathbf{C}^{-1}\otimes\mathbf{C}^{-1}-2\overline{U}'(J)J\left[\mathbf{C}^{-1}\otimes\mathbf{C}^{-1}\right]^{T_{23}}. \tag{11}$$

The particular transposition T_{23} of the fourth order tensor is defined by the transposition of the second and third index, $\mathcal{A}^{T_{23}}=a^{ikjl}\vec{g}_i\otimes\vec{g}_j\otimes\vec{g}_k\otimes\vec{g}_l$. The push-forward operation of the material tangent onto the spatial tangent operator leads to

$$\mathcal{C}=\frac{1}{J}\mathcal{F}\tilde{\mathcal{C}}\mathcal{F}^T=\left(\overline{U}''(J)J+\overline{U}'(J)\right)\mathbf{I}\otimes\mathbf{I}-2\overline{U}'(J)\mathcal{I}= \tag{12}$$

$$=\left(U''(J)J+U'(J)\right)\mathbf{I}\otimes\mathbf{I}-2\left(U'(J)+\frac{\mu}{J}\right)\mathcal{I}, \tag{13}$$

where use is made of the properties

$$[\mathbf{A}\otimes\mathbf{B}]^{T_{23}}\,\mathbf{C} = \mathbf{A}\mathbf{C}\mathbf{B}^T \tag{14}$$

$$\left[[\mathbf{A}\otimes\mathbf{B}]^{T_{23}}\right]^T = \left[\mathbf{A}^T\otimes\mathbf{B}^T\right]^{T_{23}} \tag{15}$$

$$[\mathbf{A}\otimes\mathbf{B}]^{T_{23}}\,[\mathbf{C}\otimes\mathbf{D}] = \left[[\mathbf{A}\otimes\mathbf{B}]^{T_{23}}\,\mathbf{C}\otimes\mathbf{D}\right] = \left[\mathbf{A}\mathbf{C}\mathbf{B}^T\otimes\mathbf{D}\right] \tag{16}$$

$$[\mathbf{C}\otimes\mathbf{D}]\,[\mathbf{A}\otimes\mathbf{B}]^{T_{23}} = \left[\mathbf{C}\otimes\left[\mathbf{A}^T\otimes\mathbf{B}^T\right]^{T_{23}}\,\mathbf{D}\right] = \left[\mathbf{C}\otimes\mathbf{A}^T\mathbf{D}\mathbf{B}\right] \tag{17}$$

$$[\mathbf{A}\otimes\mathbf{B}]^{T_{23}}\,[\mathbf{C}\otimes\mathbf{D}]^{T_{23}} = [\mathbf{A}\mathbf{C}\otimes\mathbf{B}\mathbf{D}]^{T_{23}}\,. \tag{18}$$

$\mathbf{A}$, $\mathbf{B}$, $\mathbf{C}$, and $\mathbf{D}$ are second order tensors.

In the small strain case, $\mathbf{F}\to\mathbf{I}$, the tangent operator reads

$$\mathcal{C}_{\mathrm{L}} = \Lambda\mathbf{I}\otimes\mathbf{I} + 2\mu\mathcal{I} = \mathcal{C}_{\mathbf{F}=\mathbf{I}} = \left(\overline{U}''(1) + \overline{U}'(1)\right)\mathbf{I}\otimes\mathbf{I} - 2\overline{U}'(1)\mathcal{I} \tag{19}$$

($\mathcal{I} = [\mathbf{I}\otimes\mathbf{I}]^{T_{23}}$ denotes the fourth order identity tensor), i.e. the Lame constants Λ and μ of small strain linear elasticity have the form

$$\Lambda = \overline{U}''(1) + \overline{U}'(1) = U''(1) + U'(1) \tag{20}$$

$$\mu = -\overline{U}'(1) \qquad\quad = -U'(1) + \mu \tag{21}$$

which restricts the form of the strain-energy function $\overline{U}(J)$, see Eq.(3), because $U'(1) = 0$ has to hold due to Eq.(21). Thus, Eq.(20) reads $\Lambda = U''(1)$. At first sight, any function $U(J)$ with the property $\Lambda = U''(1)$, $U(1) = 0$, and $U'(1) = 0$ could be chosen. However, not all of these models might yield physically ideal slopes so that it must be recommended to investigate each new proposal very carefully.

3 Simple homogeneous deformations

In the following, a number of models are investigated in view of simple shear and uniaxial tension-compression behavior. The advantage of these examples is that they might yield analytical or half-analytical expressions which are useful for both the study of the principal physical model behavior and for verifying, for example, a finite element implementation of the model. Here, three models are investigated, namely the

1. original model of [Simo and Pister, 1984]

$$U(J) = \frac{\Lambda}{2}(\ln J)^2, \quad U'(J) = \Lambda\frac{\ln J}{J}, \quad U''(J) = \Lambda\frac{1-\ln J}{J^2}, \tag{22}$$

called *Model 1*,

2. the model of [Simo and Taylor, 1991] called *Model 2*, which is defined by the ansatz

$$U(J) = \frac{\Lambda}{2}\left(\frac{J^2}{2} - \ln J - \frac{1}{2}\right), \tag{23}$$

$$U'(J) = \frac{\Lambda}{2}\left(J - \frac{1}{J}\right), \tag{24}$$

$$U''(J) = \frac{\Lambda}{2}\left(1 + \frac{1}{J^2}\right), \tag{25}$$

see fifth row of Tab. 1, and

3. the model of [Hartmann and Neff, 2003] reading

$$U(J) = \frac{\Lambda}{50}\left(J^5 + J^{-5} - 2\right), \tag{26}$$

$$U'(J) = \frac{\Lambda}{10}\left(J^4 - J^{-6}\right), \tag{27}$$

$$U''(J) = \frac{\Lambda}{10}\left(4J^3 + 6J^{-7}\right) \tag{28}$$

see last row of Tab. 1, which is defined as *Model 3*.

3.1 Simple shear

The case of simple shear defines a homogeneous deformation of the form $x = X + \kappa Y$, $y = Y$, and $z = Z$ leading to the deformation gradient

$$\mathbf{F} = \begin{bmatrix} 1 & \kappa & \\ & 1 & \\ & & 1 \end{bmatrix} \vec{\mathrm{e}}_i \otimes \vec{\mathrm{e}}_j, \qquad J = \det \mathbf{F} = 1, \tag{29}$$

and, accordingly, the left Cauchy-Green tensor takes the form

$$\mathbf{B} = \begin{bmatrix} 1+\kappa^2 & \kappa & \\ \kappa & 1 & \\ & & 1 \end{bmatrix} \vec{\mathrm{e}}_i \otimes \vec{\mathrm{e}}_j. \tag{30}$$

Fig. 1 shows the geometry and the stress boundary conditions concerned. The components of the Cauchy stress

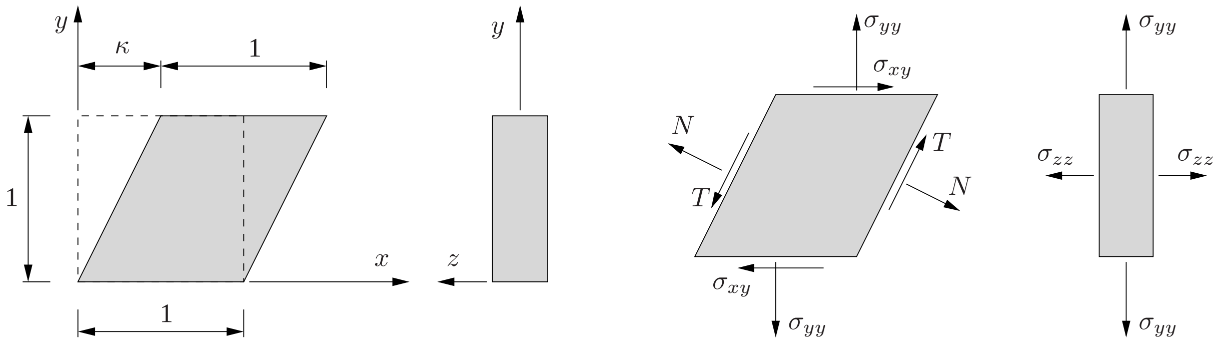

(a) Geometry (b) Stress boundary conditions

Figure 1: Simple shear

tensor (9) read

$$\sigma_{xy} = \mu\kappa, \tag{31}$$

$$\sigma_{xx} = \overline{U}'(1) + \mu(1+\kappa^2) = \mu\kappa^2, \tag{32}$$

$$\sigma_{yy} = \sigma_{zz} = \overline{U}'(1) + \mu = 0 \tag{33}$$

for the given geometrical quantities (29) and (30). Surprisingly, the stresses σ_{yy} and σ_{zz} are zero, which is independent of the magnitude of the shear parameter κ, see Eq.(3) for $J = 1$. In other words, independently of the magnitude of the shear parameter κ there are neither normal stresses in y-direction nor normal stresses in z-direction, which might be of sense in the case of a small strain theory. However, in the case of finite deformations it is more than questionable that, although a "plane strain problem" is treated, no stresses σ_{yy} and σ_{zz} occur to guarantee the geometrical constraints in thickness and vertical direction. This holds for all Simo & Pister-type models.

The simple shear problem is useful, for example, for verifying a finite element code both for a new elements of a new constitutive model. In the simple shear case the computations might be conducted using plane strain conditions of Fig. 2(a) using plane elements or three-dimensional hexahedrals, or using the boundary conditions depicted in Fig. 2(b) for three-dimensional elements. In the latter case of Fig. 2 the strain-energy function $U(J)$, or more precisely the parameter Λ, controls the closeness to the analytical solution, i.e. for $\Lambda \gg \mu$, the isochoric property of simple shear, $\det \mathbf{F} = 1$, is approximated.

3.2 Tension-compression behavior

In [Ehlers and Eipper, 1998] and later on in [Hartmann and Neff, 2003] strain-energy functions, which are related to the multiplicative decomposition of the deformation gradient into a volume changing and an isochoric part, are

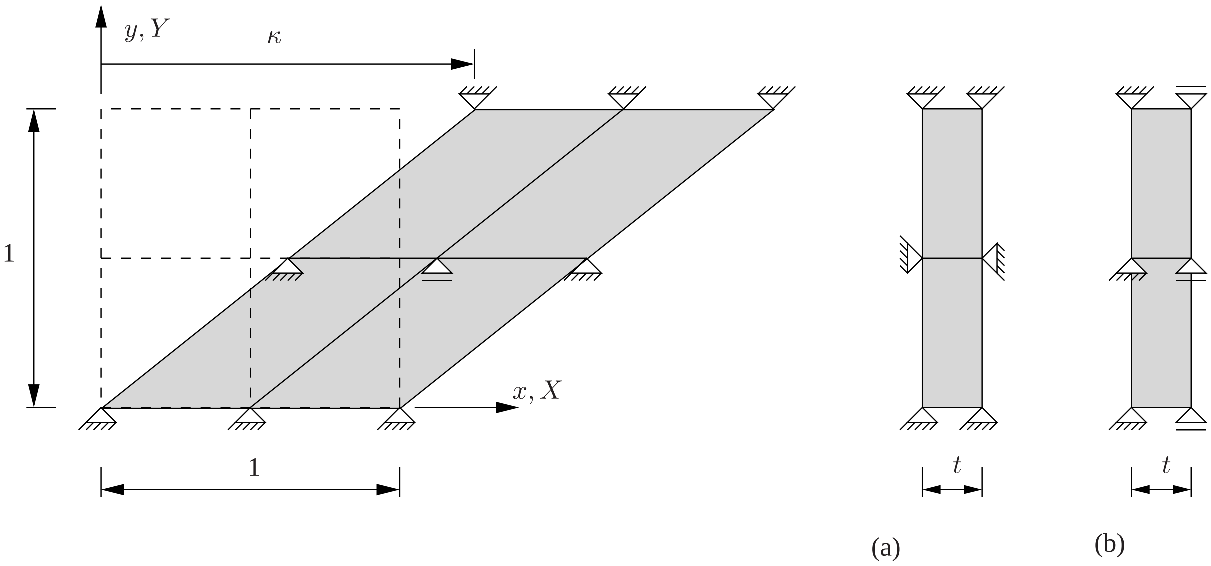

Figure 2: Four eight-noded volumetric elements and their boundary conditions in the case of simple shear

investigated. Most of them make use of the functions $U(J)$ shown in Tab. 1. Only for the model proposed by [Hartmann and Neff, 2003] a non-physical behavior was not observed. All other proposals in Tab. 1 may yield in tension an increasing of the thickness (or in compression a decrease of the thickness). Accordingly, every strain-energy function should be investigated in view of its physical properties or its range of applicability, particularly, for tension and compression. Since the Simo & Pister-type models are not based on the decomposition into volume changing and volume preserving deformations but having one part, $U(J)$, which depends only on the volume-changing deformation, studies are of interest.

Normally, the assumption of a uniaxial tension/compression deformation yields one non-linear equation in the case of compressible hyperelasticity, which has to be solved numerically. In the case of Cartesian coordinates, the deformation $x = \lambda X$, $y = \lambda_Q Y$, and $z = \lambda_Q Z$ is assumed leading to the deformation gradient

$$\mathbf{F} = \begin{bmatrix} \lambda & & \\ & \lambda_Q & \\ & & \lambda_Q \end{bmatrix} \vec{e}_i \otimes \vec{e}_j, \qquad J = \det \mathbf{F} = \lambda\lambda_Q^2 \tag{34}$$

and the left Cauchy-Green tensor

$$\mathbf{B} = \begin{bmatrix} \lambda^2 & & \\ & \lambda_Q^2 & \\ & & \lambda_Q^2 \end{bmatrix} \vec{e}_i \otimes \vec{e}_j. \tag{35}$$

λ symbolizes the prescribed axial stretch (current length over initial length, $\lambda = L/L_0$) and λ_Q represents the unknown lateral stretch. In respect of Eq.(9), the stress state and the lateral stretch can be obtained by the two equations

$$\sigma_{xx} = \overline{U}'(\lambda\lambda_Q^2) + \frac{\mu}{\lambda_Q^2}\lambda = U'(\lambda\lambda_Q^2) + \frac{\mu}{\lambda_Q^2}\left(\lambda - \frac{1}{\lambda}\right), \tag{36}$$

$$0 = \overline{U}'(\lambda\lambda_Q^2) + \frac{\mu}{\lambda} = U'(\lambda\lambda_Q^2) + \frac{\mu}{\lambda\lambda_Q^2}\left(\lambda_Q^2 - 1\right), \tag{37}$$

exploiting relation (3).

1. *Model 1*: Eq.(37) defines for the original Simo & Pister model representing a non-linear equation for computing the lateral stretch λ_Q. Using (22) with $(34)_2$ and representation (35) yield

$$\ln(\lambda\lambda_Q^2) = \frac{\mu}{\Lambda}(1 - \lambda_Q^2) \tag{38}$$

or, equivalently,

$$\lambda \lambda_Q^2 = \exp((1 - \lambda_Q^2)\mu/\Lambda) \tag{39}$$

for given λ. This equation can be reformulated into one equation with one unknown

$$g(\lambda_Q) = 0 \tag{40}$$

with

$$g(\lambda_Q) := \lambda \lambda_Q^2 - \exp((1 - \lambda_Q^2)\mu/\Lambda). \tag{41}$$

For a given λ the stress calculation requires the iterative solution of Eq.(40) and the subsequent insertion into Eq.(36), which reads in concrete form

$$\sigma_{xx} = \Lambda \frac{\ln(\lambda \lambda_Q^2)}{\lambda \lambda_Q^2} + \frac{\mu}{\lambda_Q^2}\left(\lambda - \frac{1}{\lambda}\right) \tag{42}$$

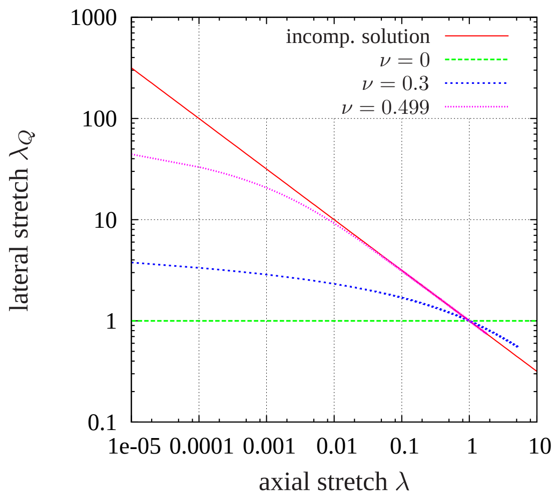

(a) model 1

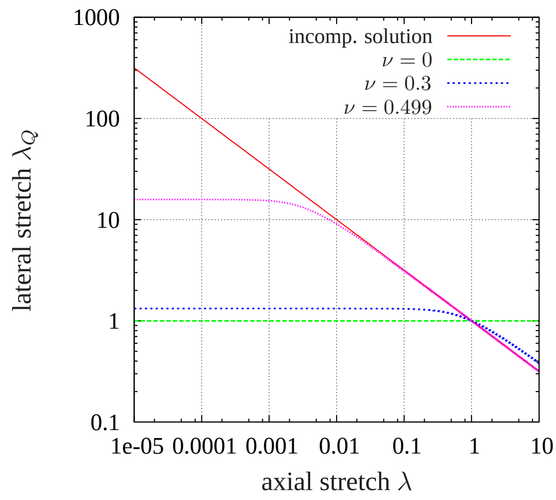

(b) model 2

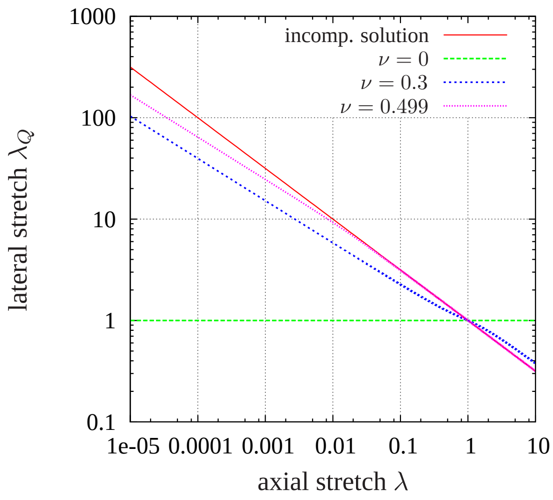

(c) model 3

Figure 3: Lateral stretch behavior for varying Lame-constant Λ and model concerned

2. *Model 2*: From Eq.(9) and by means of strain-energy (23), one obtains the two equations

$$\sigma_{xx} = \frac{\Lambda}{2}\left(\lambda\lambda_Q^2 - \frac{1}{\lambda\lambda_Q^2}\right) + \frac{\mu}{\lambda\lambda_Q^2}(\lambda^2 - 1), \tag{43}$$

$$0 = \frac{\Lambda}{2}\left(\lambda\lambda_Q^2 - \frac{1}{\lambda\lambda_Q^2}\right) + \frac{\mu}{\lambda\lambda_Q^2}(\lambda_Q^2 - 1). \tag{44}$$

The second equation is used for calculating the lateral stretch λ_Q by solving

$$\lambda_Q^2 = \frac{\mu}{\Lambda\lambda^2} \pm \sqrt{\left(\frac{\mu}{\Lambda\lambda^2}\right)^2 + \frac{\Lambda + 2\mu}{\Lambda\lambda^2}}, \tag{45}$$

i.e. we arrive at an analytical expression. Since $\lambda_Q > 0$ holds, only one solution exists.

3. *Model 3*: For model 3 defined in Eq.(26) Eq.(37) reads

$$g(\lambda_Q) = \frac{\Lambda}{10}\left((\lambda\lambda_Q^2)^4 - (\lambda\lambda_Q^2)^{-6}\right) + \frac{\mu}{\lambda\lambda_Q^2}(\lambda_Q^2 - 1) = 0 \tag{46}$$

whose solution leads the axial stresses

$$\sigma_{xx} = \frac{\Lambda}{10}\left((\lambda\lambda_Q^2)^4 - (\lambda\lambda_Q^2)^{-6}\right) + \frac{\mu}{\lambda_Q^2}(\lambda - \frac{1}{\lambda}). \tag{47}$$

Accordingly, only for specific strain-energy functions of Tab. 1 pure analytical solutions are possible.

In the following the chosen models are investigated. For the subsequent investigations use is made of a "shear modulus" $\mu = 2$ MPa. Exploiting a Poisson-ratio $\nu = 0, 0.3, 0.499$ yields for $\Lambda = 2\mu\nu/(1-2\nu)$ the Lame constant $\Lambda = 0.0, 3.0, 998.0$ MPa. In Fig. 3 the lateral stretch behavior is compared for the three different models (41), (45) and (46). The Simo & Pister model, model 1, yields a non-convergent solution for $\nu = 0.3$ between $\lambda = 2$ and $\lambda = 3$. The reason of it might come from the property that $U(J)$ is non-convex at $J > e = 2.718\ldots$. The Simo & Taylor model, model 2, does not reflect incompressibility, which commonly is tried to be incorporated with a large Λ. In all figures the relation between the lateral stretch and the axial stretch for an isochoric deformation $\det \mathbf{F} = \lambda\lambda_Q^2 = 1$, i.e. $\lambda_Q = \lambda^{-1/2}$, is depicted. The model of [Hartmann and Neff, 2003], model 3, enforces the constraint most strongly.

However, if the stress-stretch behavior is looked at, see Fig. 4, the differences can only be seen at higher stretch

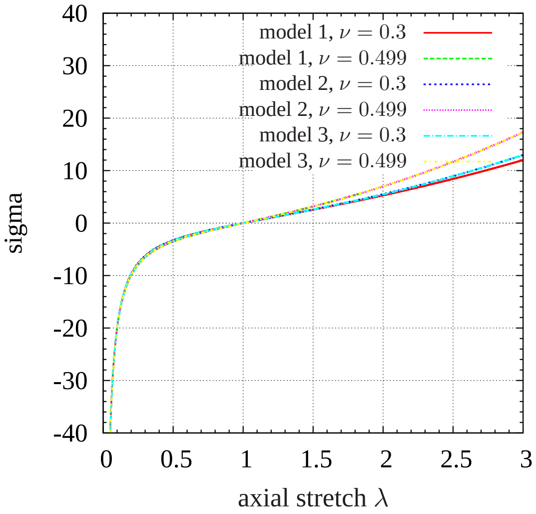

Figure 4: Stress-stretch behavior for varying Lame-parameter Λ.

magnitudes, and then, only for the differences between the magnitude of the Lame-constant Λ.

4 Conclusions

The main advantage of the Simo & Pister-type finite strain hyperelasticity relation is its simplicity represented by two material parameters which can be interpreted as the two Lame-constants occurring in linear elasticity. Accordingly, for finite deformations within a theory of metal plasticity this class of models seem to be appropriate. Particularly, the monotonous behavior in a stress-stretch diagram of a uniaxial tension-compression test seemingly yield a physical reasonable response.

However, the investigation of simple shear shows an essential drawback. There are no normal stresses in out-of-plane direction and no stresses to hold the sheared specimen perpendicular to the shear direction, which is physical unreasonable leading to non-existing second-order effects.

References

[ANSYS, 2000] ANSYS (2000). *ANSYS Theory Manual, Release 5.6*. Ansys Inc., Canonsburg.

[Ehlers and Eipper, 1998] Ehlers, W. and Eipper, G. (1998). The simple tension problem at large volumetric strains computed from finite hyperelastic material laws. *Acta Mechanica*, 130:17–27.

[Hartmann, 2002] Hartmann, S. (2002). Computation in finite strain viscoelasticity: finite elements based on the interpretation as differential-algebraic equations. *Computer Methods in Applied Mechanics and Engineering*, 191(13-14):1439–1470.

[Hartmann and Neff, 2003] Hartmann, S. and Neff, P. (2003). Polyconvexity of generalized polynomial-type hyperelastic strain energy functions for near-incompressibility. *International Journal of Solids and Structures*, 40(11):2767–2791.

[Haupt, 2002] Haupt, P. (2002). *Continuum Mechanics and Theory of Materials*. Springer, Berlin, 2 edition.

[Lion, 1996] Lion, A. (1996). A constitutive model for black filled rubber. experimental investigations and mathematical representations. *Journal of Continuum Mechanics and Thermodynamics*, 8:153–169.

[Liu et al., 1994] Liu, C. H., Hofstetter, G., and Mang, H. A. (1994). 3d finite element analysis of rubber-like materials at finite strains. *Engineering Computations*, 11:111–128.

[Lührs et al., 1997] Lührs, G., Hartmann, S., and Haupt, P. (1997). On the numerical treatment of finite deformations in elastoviscoplasticity. *Computer Methods in Applied Mechanics and Engineering*, 144:1–21.

[Miehe, 1994] Miehe, C. (1994). Aspects of the formulation and finite element implementation of large strain isotropic elasticity. *International Journal for Numerical Methods in Engineering*, 37:1981–2004.

[Murnaghan, 1951] Murnaghan, F. D. (1951). *Finite Deformation of an Elastic Solid*. Chapmann and Hall, New York.

[Ogden, 1972] Ogden, R. W. (1972). Large deformation isotropic elasticity - on the correlation of theory and experiment for compressible rubberlike solids. *Proceedings of the Royal Society of London*, Series A 328:567–583.

[Ogden, 1984] Ogden, R. W. (1984). *Non-Linear Elastic Deformations*. Ellis Horwood, Chichester.

[Reese and Govindjee, 1998] Reese, S. and Govindjee, S. (1998). A theory of finite viscoelasticity and numerical aspects. *International Journal of Solids and Structures*, 35:3455–3482.

[Roache, 1998] Roache, P. J. (1998). *Verification and validation in computational science and engineering*. Hermosa Publ., Albuquerque.

[Schwer, 2001] Schwer, L. (2001). Constitutive model verification and validation. http://www.mech.northwestern.edu/fac/cao/nsfworkshop/briefs/Schwer_p1.pdf.

[Simo and Pister, 1984] Simo, J. C. and Pister, K. S. (1984). Remarks on rate constitutive equations for finite deformation problems: Computational implications. *Computer Methods in Applied Mechanics and Engineering*, 46:201–215.

[Simo and Taylor, 1982] Simo, J. C. and Taylor, R. L. (1982). Penalty function formulations for incompressible nonlinear elastostatics. *Computer Methods in Applied Mechanics and Engineering*, 35:107–118.

[Simo and Taylor, 1991] Simo, J. C. and Taylor, R. L. (1991). Quasi-incompressible finite elasticity in principal stretches. continuum basis and numerical algorithms. *Computer Methods in Applied Mechanics and Engineering*, 85:273–310.

[Simo et al., 1985] Simo, J. C., Taylor, R. L., and Pister, K. S. (1985). Variational and projection methods for the volume constraint in finite deformation elasto-plasticity. *Computer Methods in Applied Mechanics and Engineering*, 51:177–208.

[Truesdell and Noll, 1965] Truesdell, C. and Noll, W. (1965). *The Non-Linear Field Theories of Mechanics*, volume III/3 of *Encyclopedia of Physics*. Springer Verlag, Berlin.